Complex Inorganic Solids

Structural, Stability, and Magnetic Properties of Alloys

A publication of the Third International Alloy Conference (IAC-3)

Complex Inorganic Solids

Structural, Stability, and Magnetic Properties of Alloys

Edited by

Patrice E. A. Turchi
Lawrence National Laboratory
Livermore, California

Antonios Gonis
Lawrence National Laboratory
Livermore, California

Krishna Rajan
Materials Science and Engineering Department
and Information Technology Program
Rensselaer Polytechnic Institute
Troy, New York

and

Annemarie Meike
Lawrence National Laboratory
Livermore, California

Springer

Proceedings of Third International Alloy Conference (IAC-3), held June 30–July 5, 2002 in Estoril Sol, Portugal

ISBN-10: 0-387-24811-0 (HB)
ISBN-13: 978-0387-24811-0

Printed in the United States of America

9 8 7 6 5 4 3 2 1

springeronline.com

Chairpersons/Organizers of IAC-3

TURCHI, PATRICE E. A.
Lawrence Livermore Nat'l Laboratory
C&MS, L-353
P.O. Box 808
Livermore, CA 94551, USA
Tel.: 925-422-9925
Fax: 925-423-7040
Email: turchi1@llnl.gov

RAJAN, KRISHNA
Rensselaer Polytechnic Institute
Acad. Sci. of the Mater. Sci. & Eng.
110 8th Street
Troy, NY 12180-3590, USA
Tel.: 518-276-6126
Fax: 518-276-8554
Email: rajanjk@rpi.edu

GONIS, ANTONIOS
Lawrence Livermore Nat'l Laboratory
C&MS, L-371
Livermore, CA 94551, USA
Tel.: 925-422-7150
Fax: 925-423-7040
Email: gonis1@llnl.gov

MEIKE, ANNEMARIE
Lawrence Livermore Nat'l Laboratory
L-201
Livermore, CA 94551, USA
Tel.: 925-422-3735
Fax: 925-423-8988
Email: meike1@llnl.gov

List of Participants IAC-3

ABRIKOSOV, IGOR
Uppsala University
Angstromlaboratory
Box-530
Uppsala 75121, Sweden
Tel.: 46-18-471-3568
Fax: 46-18-511-784
Email: Igor.Abrikosov@fysik.uu.se

ARDELL, ALAN
University of California at Los Angeles
Materials Science & Engineering Dept.
Metallurgy Division
6531-G Boelter Hall
Los Angeles, CA 90095-1595, USA
Tel.: 310-825-7011
Fax: (310) 206-7353
Email: aardell@ucla.edu3

BINDER, KURT
Dipartimento Di Fisica
Johannes Gutenberg Universitat Mainz
Institut Fuer Physik
Staudinger Weg 7
Mainz D-55099, Germany
Tel.: 49-6131-3923348
Fax: 49-6131-3925441
Email: kurt.binder@uni-mainz.de

BOETTGER, BERND
ACCESS E.V.
Intzestrasse 5
Aachen D-52072, Germany
Tel.: 49-241-809-8008
Fax: 49-241-385-78
Email: b.boettger@access.rwth-aachen.de

BOETTINGER, WILLIAM
NIST
100 Bureau Dr., MS 8555
Room A153, BD 223
Gaithersburg, MD 20899, USA
Tel.: 301-975-6160
Fax: 301-975-4553
Email: wboettinger@nist.gov

BRUNO, EZIO
Universita' Di Messina
Dipartimento Di Fisica
Contrada Papardo
Salita Sperone
Messina, ME I-98166, Italy
Tel.: 39-090-393-713
Fax: 39-090-676-5042
Email: bruno@dsme01.unime.it

CHEN, YING
RACE
University of Tokyo
Komaba 4-6-1
Meguro-ku
Tokyo 153-8904, Japan
Tel.: 81-3-5453-5896
Fax: 81-3-3467-0648
Email: ying@race.u-tokyo.ac.jp

CHEPULSKII, ROMAN
National Academy of Sciences
Institute for Metal
Institute for Metal Physics
36, Acad. Vernadsky Blvd.
Kiev 142 UA-03680, Ukraine
Tel.: 380-44-444-1221
Fax: 380-44-444-2561
Email: r_chepulskii@yahoo.com

CLOUET, EMMANUEL
CEA Saclay
SRMP- Bat.520
Gif-sur-Yvette F-91191, France
Tel.: 33-1-6908-6663
Fax: 33-1-6908-6867
Email: emmanuel.clouet@cea.fr

DRCHAL, VACLAV
Institute of Physics AS CR
Na Slovance 2
Praha 8 CZ-182 21, Czech Republic
Tel.: 420-2-6605-2926
Fax: 420-2-8689-0527
Email: drchal@fzu.cz6

EIKEN, JANIN
ACCESS E.V.
Intzestrasse 5
Aachen D-52072, Germany
Tel.: 49-241-809-8009
Fax: 49-241-385-78
Email: j.eiken@access.rwth-aachen.de

EVERETT, RICHARD
Office of Naval Research IFO
223 Old Marylebone Road
London NW1 5TH, United Kingdom
Tel.: 44-207-514-4413
Fax: 44-207-723-6359
Email: reverett@onrifo.navy.mil

FAULKNER, JOHN
Florida Atlantic University
Dept. of Physics
825 Walnut Terrace
Boca Raton, FL 33486, USA
Tel.: 561-297-3429
Fax: 561-297-2662
Email: faulkner@fau.edu

FENG, YUAN
National University of Singapore
10 Science Drive 4
Lower Kent Ridge Road
Singapore 117542, Singapore
Tel.: 65-6874-2960
Fax: 65-6777-6126
Email: phyfyp@nus.edu.sg

FRIES, SUZANA
Access e.V., RWTH-Aachen
Intzestrasse 5
Aachen D-52072, Germany
Tel.: 49-241-809-8013
Fax: 49-241-385-78
Email: sufries@mf.mpg.de

GAUNE-ESCARD, MARCELLE
Ecole Polytechnique
IUSTI-UMR 6595 CNRS
5 Rue Enrico Fermi
Marseille F-13453, France
Tel.: 33-4-9110-6887
Fax: 33-4-9111-7439
Email: Marcelle.Gaune-Escard@polytech.univ-mrs.fr

GONIS, ANTONIOS
Lawrence Livermore Nat'l Laboratory
C&MS, L-371
Livermore, CA 94551, USA
Tel.: 925-422-7150
Fax: 925-423-7040
Email: gonis1@llnl.gov

GRIMVALL, GORAN
Royal Institute of Technology
KTH-SCFAB
Theory of Materials
Stockholm SE-106 91, Sweden
Tel.: 46-8-5537-8160
Fax: 46-8-5537-8470
Email: grimvall@theophys.kth.se

GUY, BERNARD
Ecole des Mines
158 Cours Fauriel
Saint-Etienne F-42023, France
Tel.: 33-4-7742-0164
Fax: 33-4-7742-0000
Email: guy@emse.fr

HATA, SATOSHI
Kyushu University
Interdisc. Grad. School of Eng. Sci.
6-1 Kasugakouen
Kasuga, Fukuoka 816-8580, Japan
Tel.: 81-92-583-7536
Fax: 81-92-575-2318
Email: hata@asem.kyushu-u.ac.jp

HAYES, FRED
University of Manchester
Materials Science Centre
Grosvenor Street
Manchester M1 7HS, United Kingdom
Tel.: 44-161-200-3566
Fax: 44-161-200-3586
Email: fred.hayes@umist.ac.uk

HEHENKAMP, THEODOR
Georg-August Univ. Gottingen
Institut fur Metallphysik
Hospitalstrasse 3-7
Gottingen D-37073, Germany
Tel.: 49-551-794-903
Fax: 49-551-395-012

HICKERNELL, BARBARA
Engineering Conferences International
3 Park Avenue
27th Floor
New York, NY 10016-5902, USA
Tel.: 1-212-591-7836
Fax: 1-212-591-7441
Email: engfnd@aol.com

KAUFMAN, LARRY
M.I.T.
140 Clark Road
Brookline, MA 02445-5848, USA
Tel.: 617-731-2622
Fax: 617-566-70967
Email: larrykaufman@rcn.com

KHACHATURYAN, ARMEN
Rutgers University
Dept. of M.S. & E.
607 Taylor Road
Piscataway, NJ 08855-0909, USA
Tel.: 732-445-4711
Fax: 732-445-6780
Email: khach@jove.rutgers.edu

KLEIN, BARRY
University of California -Davis
One Shields Avenue
402 Mrak Hall
Davis, CA 95616-8671, USA
Tel.: 530-752-4091
Fax: 530-752-0602
Email: bmklein@ucdavis.edu

KORZHAVYI, PAVEL
Royal Inst. of Technology (KTH)
Materials Science & Engineering
Brinellvaegen 23
Stockholm SE-100 44, Sweden
Tel.: 46-8-790-8832
Fax: 46-8-207-681
Email: pavel@met.kth.se

KUDRNOVSKY, JOSEF
Institute of Physics AS CR
Na Slovance 2
Prague 8 CZ-182 21, Czech Republic
Tel.: 420-2-6605-2905
Fax: 420-2-821-227
Email: kudrnov@fzu.cz

LE BOUAR, YANN
LEM-CNRS
29 Avenue De La Division Leclerc
BP 72
Chatillon F-92322, France
Tel.: 33-1-4673-4592
Fax: 33-1-4673-4155
Email: lebouar@onera.fr

MASUDA-JINDO, KINICHI
Tokyo Institute of Technology
Material Science Department
Nagatsuta 4259, Midori-ku
Yokohama, Kanagawa 226-8503, Japan
Tel.: 81-45-924-5636
Fax: 81-424-75-0650
Email: wmfjindo@din.or.jp

MAUGIS, PHILIPPE
IRSID - Arcelor Group
Voie Romaine - BP 30320
Maizieres-les-Metz F-57283, France
Tel.: 33-387-704779
Fax: 33-387-704712
Email:
philippe.maugis@irsid.usinor.com

MEIKE, ANNEMARIE
Lawrence Livermore Nat'l Laboratory
L-201
Livermore, CA 94551, USA
Tel.: 925-422-3735
Fax: 925-423-8988
Email: meike1@llnl.gov

MENON, MADHU
University of Kentucky
Physics Department
Lexington, KY 40506, USA
Tel.: 859-257-8737
Fax: 859-323-1029
Email: madhu@ccs.uky.edu4

MILICI, ANTONIO
Graduate Student
University of Messina
Department of Physics
Contrada Papardo Salita Sperone
Messina I-98166, Italy
Tel.: 39-090-393-713
Fax: 39-090-676-5042
Email: amilici@dsme01.unime.it

MOHRI, TETSUO
Hokkaido University
Graduate School of Engineering
Kita-13, Nishi-8, Kita-ku
Sapporo 060-8628, Japan
Tel.: 81-11-706-6348
Fax: 81-11-706-6348
Email: tmohri@eng.hokudai.ac.jp

NISHIZAWA, SHUICHI
Tohoku University
Aramaki-Aza-Aoba
Aoba-Ku 01
Sendai, Miyagi 980-8579, Japan
Fax: 81-22-217-6903

PENTCHEVA, ROSSITZA
University of Munich
Inst. of Crytallography
Theresienstrasse 41
Munich D-80333, Germany
Tel.: 49-89-2180-4352
Fax: 49-89-2180-4334
Email: pentcheva@lrz.uni-muenchen.de

PFEILER, WOLFGANG
University of Vienna
Institut fur Materialphysik
Strudlhofgasse 4
Vienna A-1090, Austria
Tel.: 43-1-4277-51309
Fax: 43-1-42-779-513
Email: pfeiler@ap.univie.ac.at

RAJAN, KRISHNA
Rensselaer Polytechnic Institute
Acad. Sci. of the Mater. Sci. & Eng.
110 8th Street
Troy, NY 12180-3590, USA
Tel.: 518-276-6126
Fax: 518-276-8554
Email: rajank@rpi.edu

RUBAN, ANDREI
Tech. University of Denmark
CAMP, Physics Department
Bldg. 307
Lyngby 2800, Denmark
Tel.: 45-4525-3234
Fax: 45-4593-2399
Email: ruban@fysik.dtu.dk

SAITO, YOSHIYUKI
Waseda University
Dept. of Mater. Sci. & Eng.
3-4-1 Okubo
Shinjuku-ku
Tokyo 169-8555, Japan
Tel.: 81-3-5286-3314
Fax: 81-3-5286-3314
Email: ysaito@mn.waseda.ac.jp

SIBERCHICOT, BRUNO
CEA/DAM-DIF
BP 12
Bruyeres-le-Chatel F-91680, France
Tel.: 39-01-6926-7327
Fax: 39-01-6926-7077
Email: bruno.siberchicot@cea.fr

SOB, MOJMIR
Institute of Physics of Materials
Zizkova 22
Brno CZ-616 62, Czech Republic
Tel.: 420-5-3229-0455
Fax: 420-5-4121-2301
Email: mojmir@ipm.cz

STOLOFF, NORMAN
Rensselaer Polytechnic Institute
Materials Sci. & Engrg. Dept.
Troy, NY 12180-3590, USA
Tel.: 518-276-6436
Fax: 518-276-8554
Email: stolon@rpi.edu

THIBAUDEAU, PASCAL
C.E.A./Le Ripault
BP 16
Monts F-37160, France
Tel.: 33-247-344-656
Fax: 33-247-345-154
Email: pascal.thibaudeau@cea.fr

TURCHI, PATRICE E. A.
Lawrence Livermore Nat'l Laboratory
C&MS, L-353
P.O. Box 808
Livermore, CA 94551, USA
Tel.: 925-422-9925
Fax: 925-423-7040
Email: turchi1@llnl.gov

VAKS, VALENTIN
RRC Kurchatov Institute
Kurchatov Square 1
Moscow 123182, Russia
Tel.: 7-095-1969826
Fax: 7-095-8825804
Email: vaks@mbslab.kiae.ru

WATANABE, TADAO
Tohoku University
Aramaki-Aza-Aoba
Aoba-Ku 01
Sendai Miyagi 980-8579, Japan
Tel.: 81-22-217-6902
Fax: 81-22-217-6903
Email:
watanabe@mdie.mech.tohoku.ac.jp

WONG, JOE
Lawrence Livermore Nat'l. Laboratory
C&MS, L-356
P.O. Box 808
Livermore, CA 94551, USA
Tel.: 925-423-6385
Fax: 925-424-4737
Email: wong10@llnl.gov

WUENSCH, BERNHARDT
M.I.T.
Ceramics Division 13-4037
77 Massachusetts Avenue
Cambridge, MA 02139-4307, USA
Tel.: 617-253-6889
Fax: 617-253-5827
Email: wuensch@mit.edu

ZINGALES, LEON
University of Messina
Department of Physics
Salita Sperone Contrada Papardo
Messina I-98166, Italy
Tel.: 39-090-393-713
Fax: 39-090-676-5042
Email: zingales@dsme01.unime.it

PREFACE

This volume contains the proceedings of the Third International Alloy Conference (IAC-3) that was held in Estoril Sol, Lisbon, Portugal, June 30-July 5, 2002. Like its predecessors, and anticipated for those planned for the future, the conference brought together experimental and theoretical/computational scientists involved in the study of alloys taken to mean (solid) materials composed of more than one chemical species.

The study of alloys involves two main but interrelated areas of science: First, the determination of the electronic states in a material and the effect of these states on properties, and second the thermodynamic behavior of the materials as it arises in the study of phase transformation and phase evolution in time. Properties like formation energy, electronic transport, magnetism, and mechanical behavior are intimately tied into the nature of electronic states. Kinetics of transformation, phase evolution and aging are the subject of thermodynamics. Both kinds of properties, however, are interconnected in that information extracted from one study is often applicable to the other.

The papers presented in the conference span the spectrum of activity in the science of alloys. The theoretical presentations ranged in content from fundamental studies of electronic structure, to first-principles calculations of phase diagrams, to the effects of charge transfer, to the temperature dependence of short-range order parameters. They encompassed the study of mechanical properties, the properties of dislocations, of phase evolution, and computer simulations. Experimental studies were presented based on a variety of state of the art experimental techniques, from TEM to synchrotron diffraction. The phenomena studied varied from the precipitation of nitrides in steel, to the wetting of interfaces between two different crystal structures, to the ordering of vacancies in carbides. And the materials whose properties were measured ranged from Transition metals, to the Lanthanides, to the Actinide series of compounds and alloys.

The third conference in the series confirmed, as if there were any doubt, the richness and complexity of phenomena that is embodied in the physics of alloys. An incredible amount of effort combining experimental and theoretical aspects is continuously expended in the attempt to understand this physics and it in a productive way in engineering applications. This intensive effort points toward the importance of understanding and predicting alloy properties but also to the challenging nature of the task.

There is good reason for hoping that significant progress is in the making, however. Recent developments in the theory of studying correlations in fluctuating systems have emerge with a

fresh air of unifying power that encompasses both alloys and the Coulomb interaction in solids. We are looking forward to the next International Alloy Conference to hear more about these developments and to record them for the scientific community. Interface between *ab initio* and phenomenological modeling of alloy properties, with predictive tools to help the design of new materials with engineering requirements is another topic that is taking momentum and will certainly be discussed more at the next IAC.

In organizing the IAC-3, we are grateful to our sponsors both for financial assistance and for organizational aid. The U. S. Army Research Office Physics Division, the Materials Research Institute at Lawrence Livermore National Laboratory, the U.S. Office of Naval Research Materials Division, and the United Engineering Foundation, our main and official sponsors were forthcoming with generous financial contributions. The UEF also provided the logistics and the administrative components of bringing together a significant number of alloy scientists to a magnificent place in Portugal. As organizers we can only express our deep appreciation to them for these efforts.

At last but certainly not least, the staff at Kluwer/Plenum contributed their expertise along with a great exercise of patience in the production of this volume. Because of their efforts the volumes in the series now begin to take the form of a unified work, a feature that will be augmented, as more volumes become available. We thank them and hope that well continue our fruitful collaboration for a long time into the future.

P. E. A. Turchi
A. Gonis
K. Rajan
A. Meike

CONTENTS

KINETICS, DIFFUSION AND TRANSPORT

MAGNETIC AND ELASTIC PROPERTIES

THEORY

MICROSTRUCTURAL PROPERTIES

PRECIPITATION OF DISORDERED Ni-X SOLID SOLUTION PHASES IN OFF-STOICHIOMETRIC ORDERED Ni_3X ALLOYS

Y. Ma[1], J. Joshi[2] and A.J. Ardell[1]

[1]Department of Materials Science and Engineering
University of California, Los Angeles, CA 90095-1595, USA
[2]Aaj Accumulators Pvt. Ltd., W–54 M.I.D.C.
Shiroli. Tal. Hatkanagale, India 416 122

INTRODUCTION

The coarsening behavior of coherent γ precipitates (Ni-X solid solution, X = Al, Ge or Ga) in a matrix of the off-stoichiometric γ' phase (Ni_3X) is currently under investigation in binary Ni-Al, Ni-Ge and Ni-Ga alloys. Of particular interest are the evolution of the precipitate microstructure (morphology and spatial correlations), the scaling behavior of the particle size distributions and the kinetics of coarsening and its dependence on volume fraction. Since the compositions and temperatures of greatest interest are very close to the (γ + γ')/γ' phase boundary, hereafter called the γ solvus, we need to locate it as accurately as possible in each alloy. The γ solvus is retrograde in binary Ni-Al, Ni-Ge and possibly Ni-Ga alloys, but is not known with precision for any of the 3 alloys. In Ni-Al alloys there is a minimum retrograde solubility of ~22 at. % somewhere between 1000 and 1200 °C, but there is considerable scatter in the published data[1-4], as shown in Fig.1. The uncertainty is unacceptably large for our purposes.

Depending on composition, either isothermal aging or continuous cooling of hypostoichiometric Ni_3X produces precipitates of the γ phase. Cornwell and Purdy[5] stated that the γ precipitates in binary Ni-Al alloys were plate-shaped and coherent. However, Liu et al.[6] reported that the precipitate particles in a quaternary alloy were initially spherical and evolved with aging time to cuboidal shapes, becoming plate-like only at longer aging times. In the reverse system, i.e. γ' precipitates in γ matrix, the γ' precipitates evolve in shape from spheres to cuboids to nearly perfect cubes[7], and can become concave cuboids (cuboids with concave interfaces) at large sizes if the volume fraction is small enough (< 0.04 or so)[8,9]. Plate-shaped γ' precipitates usually form as a result of coalescence[7]. One immediate question of interest is why the morphological evolution of γ' in γ should be different from that of γ in γ'. After all, the interfacial free energy is independent of which is the minority or majority phase, and so are the elastic self- and interaction energies. To be sure, the lattice and elastic-constant mismatches are reversed in sign, but they are identical

in magnitude. Since elastic energies are proportional to the square of the lattice and elastic constant mismatches, their signs should not matter.

Other important issues involve comparisons of the kinetics of coarsening of the two phases in each other, and how the coarsening kinetics of γ in γ' depend on volume fraction; the dependence is anomalous for the reverse system[10]. In this paper we present some of the preliminary results of our research. Most of the results to date are on Ni-Al alloys, and the majority of the paper concentrates on these. Nevertheless some information has also been obtained on precipitation in Ni_3Ge and Ni_3Ga alloys, and these results are also briefly mentioned.

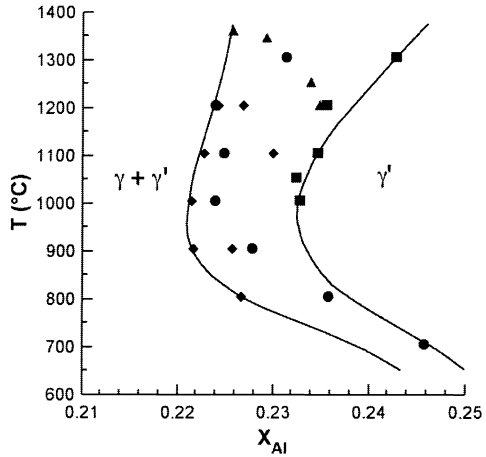

Figure 1. Illustrating the uncertainty in the precise position of the γ solvus (the boundary between the $\gamma + \gamma'$ and γ' regions in the Ni-Al phase diagram). The curves are drawn to illustrate the extremes of the range of data reported in the literature. Data of: ■ Janssen[1]; ▲ Verhoeven et al.[2]; ● Jia (cited by Okamoto[3]); ◆ Watanabe et al.[4].

EXPERIMENTAL PROCEDURES

Binary Ni-Al alloys containing 22.0, 22.2, 22.4, 22.6, 22.8 and 23.0 at. % Al were purchased from the Alloy Preparation Facility of the Ames Laboratory, Ames, IA. The alloys were arc-melted and chill cast into water-cooled Cu crucibles and delivered to us in the form of rods approximately 12 mm in diameter. Weight losses during melting and casting of the alloys were at most 0.025%, indicating that the compositions were indeed the compositions of the alloys received. The alloys were annealed in a vacuum of 3×10^{-5} torr at 1200 °C for up to 72 h in order to improve homogeneity. The compositions of the alloys were further verified using energy-dispersive x-ray spectroscopy (EDS) and inductively coupled plasma spectroscopy. We believe that the compositions reported are accurate to within ± 0.03 at. %.

Binary Ni-Ge alloys containing 22.0, 22.5, and 23.0 at. % Ge and binary Ni-Ga alloys containing 22.0, 22.5, and 23.0 at. % Ga were also purchased from the Ames Laboratory, where they were annealed in vacuum at 1000 °C for 100 h prior to shipping. Weight losses during melting and casting of these alloys were small enough to be considered negligible, so the reported compositions are taken as the true compositions.

Slices were made using electric-spark discharge machining, and after polishing were "solution treated" in an inert argon atmosphere at 1100 ± 1 °C for 1.5 h (Ni-Al alloys) or 1000 ± 1 °C for 0.75 h (Ni-Ge and Ni-Ga alloys) and quenched into refrigerated brine. These slices were aged at various temperatures and times in a vertical tube furnace, in

which the temperature fluctuated by less than ±0.5 °C. Specimens were cored from the aged slices and electrolytically polished for examination by transmission electron microscopy (TEM) using a JEOL model 100CX TEMSCAN operating at 100 kV.

Particle sizes and shapes were evaluated from dark-field images taken using a {100} superlattice reflection from thin foils in [001] orientation. Other diffracting conditions were tried, but this one produced the best contrast. The sizes and shapes of the γ precipitates were evaluated using image-analysis software. For non-equiaxed γ precipitates, the "radius", r, was defined as $(a + b + c + d)/8$, where a, b, c and d are the sides of the circumscribed polygon.

RESULTS AND DISCUSSION

Dissolution Experiments

Accurate knowledge of the γ solvus is a requirement for determining how the coarsening kinetics of γ in γ' depend on volume fraction. Simply solution-treating the alloys and aging them for various times within the expected 2-phase region of the phase diagram proved to be insufficient to establish the γ solvus. This is exemplified in Fig. 2, which shows the results of two experiments on aging the 22.6 % alloy, one at 650 °C for 240 h and the other at 700 °C for 120 h. Precipitates can be seen clearly in Fig. 2a, but none are present in Fig. 2b. These results would ordinarily lead us to conclude that the solvus temperature for the alloy containing 22.6 % Al is between 650 and 700 °C. However, if the 22.6 % Al alloy is aged first at 650 °C to produce small coherent γ precipitates, and subsequently re-aged at successively higher temperatures, we obtain completely different results. These are exemplified by the micrographs in Fig. 3. Here we observe γ precipitates in specimens re-aged to temperatures as high as 755 °C (Fig. 3c), and it is evident that complete dissolution of the γ precipitates is observed only after re-aging at 765 °C (Fig. 3d). The γ solvus for the alloy containing 22.6 % Al clearly lies between 755 and 765 °C, which is more than 50 °C higher than indicated by the microstructures shown in Fig. 2.

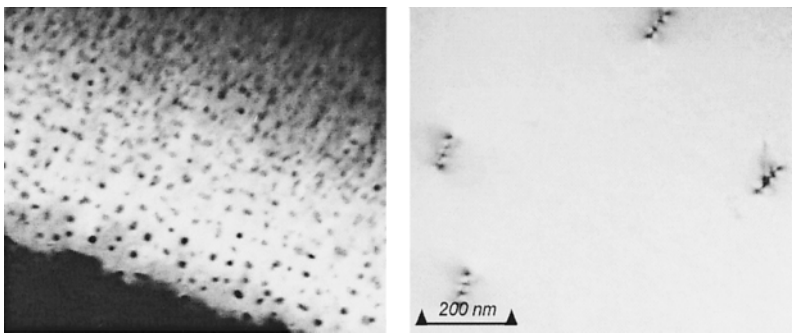

(a) (b)

Figure 2. The microstructures in the alloy containing 22.6 % Al after solution-treating and aging under the following conditions: (a) 650 °C for 240 h (b) 700 °C for 120 h.

The reason that dissolution experiments are needed to accurately determine the γ solvus is simply that nucleation of the γ phase from supersaturated γ' is much slower than nucleation of γ' from supersaturated γ[11]. The principle involved is simple. There is a large energetic barrier to nucleation of the γ phase but no barrier to their dissolution. In addition to dissolution experiments, additional work was done to determine the concentration of Al in the matrix of the alloys containing 22.0 and 22.2 % Al, wherein dendrites of the γ phase were never eliminated by annealing[12]. This work produced the γ solvus shown in Fig. 4.

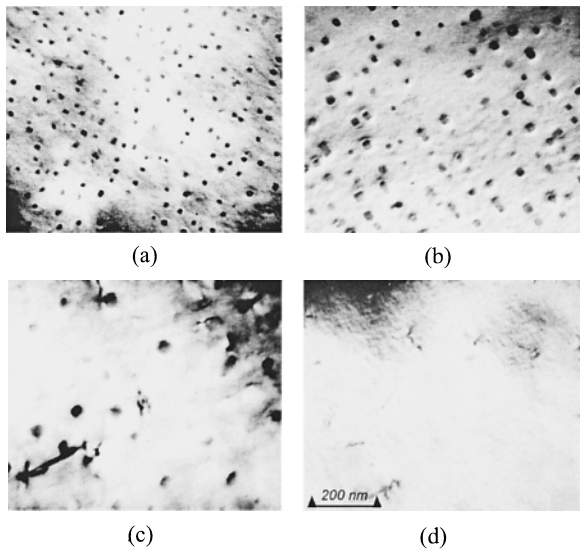

Figure 3. The microstructures in the alloy containing 22.6 % Al after solution-treating and aging under the following conditions: (a) 650 °C for 96 h plus 730 °C for 1.5 h; (b) 650 °C for 144 h plus 740 °C for 27 h; (c) 650 °C for 240 h plus 755 °C for 18 h; (d) 650 °C for 240 h plus 765 °C for 18 h.

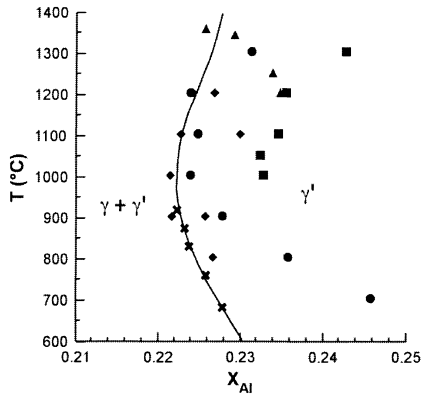

Figure 4. The γ solvus (solid curve) determined from the dissolution experiments of Ma et al.[12]. The symbol ✖ represents the solvus resulting from the dissolution experiments. The other plotting symbols are identical to those in Fig. 1.

Coarsening kinetics

Representative precipitate microstructures during precipitation of the γ phase in the 22.0 at. % Al alloy aged at 700 °C are shown in Fig. 5. The very small number of γ precipitates seen after aging for 8 h is indicative of the difficulty of their nucleation. The morphology of the γ precipitates evolves from spherical to cuboidal even when they are very small (< 50 nm in diameter), as evidenced by the presence of flat interfaces after only 48 h of aging; the flat interfaces are parallel to ⟨001⟩. Many plate-shaped precipitates are evident

after 96 h of aging despite their small size. It is not evident at this stage of the research whether the plate shape results from the breaking of equiaxed symmetry, as predicted theoretically[13], or whether adjacent γ precipitates coalesce readily, since there is no issue involving anti-phase ordering relationships, as there is for the coalescence of γ' precipitates[14]. Measurements of the sizes of the precipitates in Fig. 5 and plotting them according to the expected rate law for coarsening[15,16] i.e. $\langle r \rangle^3 \propto kt$, where k is the rate constant for coarsening and t is the aging time, leads to the results shown in Fig. 6. The linearity is quite good, indicating that the γ precipitates evidently grow by diffusion-controlled coarsening.

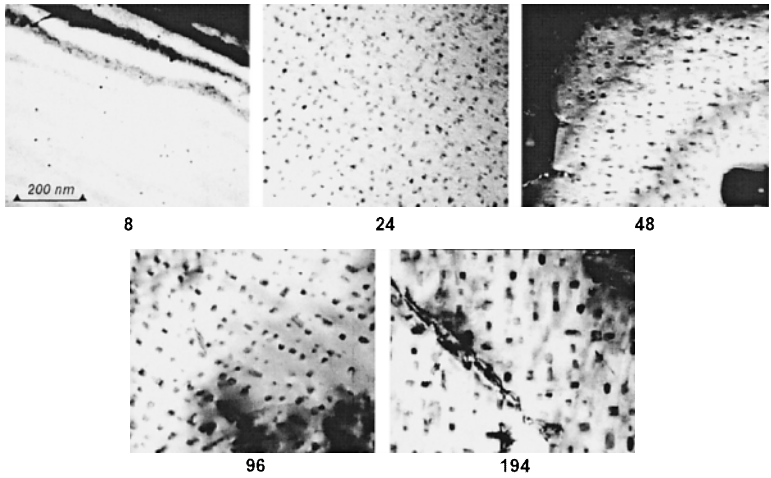

Figure 5. Evolution of precipitates in the 22.0 at % Al alloy at 700 °C. The number under each figure indicates the aging time in h.

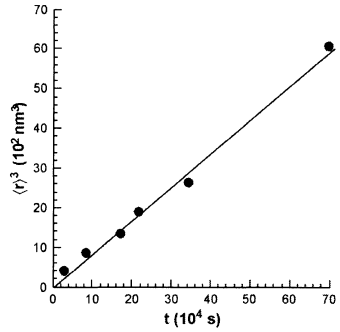

Figure 6. The kinetics of coarsening at 700 °C of the γ precipitates in the γ' matrix of the 22.0 % Al alloy, plotted as the cube of the average radius, $\langle r \rangle$, vs. aging time, t.

Figure 7 illustrates the relative rates of precipitation of γ in γ' and γ' in γ observed in a dendritic region of the alloy containing 22.0 % Al aged for 48 h at 700 °C. It is quite evident that the precipitation of γ in γ' is much slower than the precipitation of γ' in γ. This is most likely due to the faster coarsening kinetics of γ' in γ, but the slower nucleation kinetics of γ in γ' undoubtedly contribute as well. According to Calderon et al.[17], k can be expressed by the equation

$$k = \frac{8D\sigma V_{m\beta}}{9G''_{m\alpha}\left(X_{\beta e} - X_{\alpha e}\right)^2}, \tag{1}$$

where D is the coefficient of diffusion of solute in the matrix, $V_{m\beta}$ is the average volume per atomic site in the precipitate (β) phase, $X_{\alpha e}$ is the equilibrium solubility of the solute in the matrix (α) phase, $X_{\beta e}$ is the equilibrium solubility of the solute in the dispersed phase and $G''_{m\alpha}$ is the second derivative of the molar free energy of mixing of the matrix phase with respect to composition, evaluated at $X_{\alpha e}$.

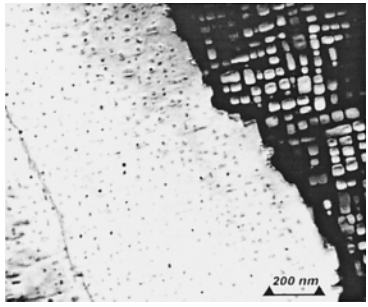

Figure 7. A dark-field TEM micrograph showing the precipitation of γ (dark) in γ' (bright) and γ' (bright) in γ (dark) in a dendritic region of the 22.0 at % Al alloy aged at 700 °C for 48 h.

During coarsening it is necessary not only to transport solute atoms to growing precipitates and away from shrinking ones, but also to transport *solvent* atoms *away* from growing precipitates and *towards* shrinking ones. Assuming that the concentration of vacancies is in equilibrium everywhere during diffusion, it is more appropriate to describe diffusion in terms of the chemical diffusion coefficient, $\tilde{D}$, which can be written as

$$\tilde{D} = S\left\{XD_B^* + (1-X)D_A^*\right\}X(1-X)\frac{G''_{m\alpha}}{RT}, \tag{2}$$

where D_A^* and D_B^* are the tracer diffusion coefficients of the solvent (A) and solute (B) a t-oms in the matrix with solute concentration X, R is the gas constant, T is the absolute temperature and S is Manning's vacancy flow factor[18], given by the general equation

$$S = 1 + \left[f_o^{-1} - 1\right]\left\{\frac{X(1-X)\left[D_A^* - D_B^*\right]^2}{\left[XD_A^* + (1-X)D_B^*\right]\left[(1-X)D_A^* + XD_B^*\right]}\right\}, \tag{3}$$

where f_o is the correlation coefficient. Applying equations (2) and (3) separately to the γ and γ' phases, and substituting them into eq. (1) allows us to express the ratio of the rate constants for the coarsening of γ' in γ and *vice versa* as

$$\frac{k_\gamma}{k_{\gamma'}} = \frac{S_\gamma\left[(1-X_{\gamma e})D^*_{Al,\gamma} + X_{\gamma e}D^*_{Ni,\gamma}\right]X_{\gamma e}(1-X_{\gamma e})}{S_{\gamma'}\left[(1-X_{\gamma' e})D^*_{Al,\gamma'} + X_{\gamma' e}D^*_{Ni,\gamma'}\right]X_{\gamma' e}(1-X_{\gamma' e})}, \tag{4}$$

where the subscripts refer to the phase, which acts as the matrix (e.g. k_γ is the rate constant for coarsening of γ' precipitates in the γ phase of equilibrium composition $X_{\gamma e}$). The molar volumes of solute have been taken as equal in eq. (4).

To compare $k_\gamma/k_{\gamma'}$ calculated using eq. (4) with experimental measurement, we analyze data on coarsening at 700 °C. The calculations make use of diffusion coefficients estimated from the sources summarized in Table 1. For the calculation of $k_\gamma/k_{\gamma'}$ we used f_o = 0.781 for diffusion in the γ phase and f_o = 0.689 for diffusion in the γ' phase[19]. The chemical diffusion coefficients are 1.016×10^{-18} m²/s and 8.030×10^{-21} m²/s for the γ and γ' phases. respectively. Experimentally, the slope of the straight line fitted to the data in Fig. 6 yields the value $k_{\gamma'} = 8.49 \times 10^{-3}$ nm³/s. From analysis of data on the coarsening of γ' precipitates[22] at 700 °C we obtain $k_\gamma = 4.23 \times 10^{-2}$ nm³/s. The ratio $k_\gamma/k_{\gamma'}$ from experiment is thus ≈5; the value calculated theoretically is 77. Possible reasons for the discrepancy are not evident, but the assumed value of $D^*_{Ni,\gamma} = D^*_{Al,\gamma}/10$ in Table 1 is an obvious candidate.

Table 1. Tracer diffusion coefficients in the γ and γ' phases.

D (m²/s)	D at 700 °C (m²/s)	Ref.
$D^*_{Al,\gamma} = 7.1\times10^{-4}\, exp\left\{\frac{-276{,}600}{RT}\right\}$	1.01×10^{-18}	20
$D^*_{Ni,\gamma} = \frac{D^*_{Al,\gamma}}{10}$	1.01×10^{-19}	--
$D^*_{Al,\gamma'} = 0.372\, exp\left\{\frac{-375{,}400}{RT}\right\}$	2.63×10^{-21}	21
$D^*_{Ni,\gamma'} = 3.31\times10^{-4}\, exp\left\{\frac{-302{,}200}{RT}\right\}$	1.99×10^{-20}	21

The Ni-Ge and Ni-Ga alloy systems

Precipitates of the Ni-Ge solid solution have been observed in the Ni_3Ge matrix in all 3 Ni-Ge alloys. Figure 8 shows the microstructures in the 22.0 % Ge alloy aged at 700 °C. The morphology changed from cuboidal to plate-like at a fairly short aging time. Observations of precipitates in dendritic regions of the 22.0 % Ge alloy indicate that precipitation of the Ni-Ge solid solution in Ni_3Ge is much slower than in the reverse system, similar to what is observed in Ni-Al alloys. Dissolution experiments are in progress to accurately establish the γ solvus in the Ni-Ge system.

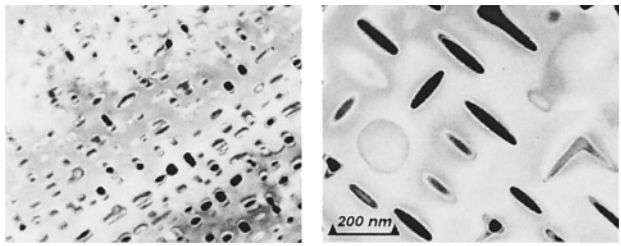

(a) (b)

Figure 8. Precipitates of the Ni-Ge solid solution in Ni_3Ge, observed in an alloy containing 22.0 at. % Ge aged for (a) 8 h and (b) 48 h at 700 °C.

Aging experiments have also been conducted on the Ni-Ga alloys at temperatures in the range 600 to 800 °C. So far we have not observed the precipitation of the solid solution phase, which indicates that the γ solvus in this alloy system does not have the necessary negative slope in the Ni-Ga phase diagram.

SUMMARY

Nucleation of the solid solution γ phase from the ordered γ' phase (Ni_3Al) is quite difficult. Undercooling the 22.6 at.% Al alloy by more than 50 °C to a temperature (700 °C) at which diffusion is reasonably rapid fails to produce observable γ precipitates, even after aging for 120 h. The phase boundary can be best found through the use of dissolution experiments, which take advantage of the absence of a barrier to the dissolution of γ phase.

The γ precipitates are equiaxed when small, then non-equiaxed as they grow and eventually become plate-like shaped. The γ precipitates transform into plates far more readily than γ' precipitates, which is attributed to the absence of anti-phase boundaries in the γ phase. Despite the non-equiaxed shapes, $\langle r \rangle^3$ depends approximately linearly on aging time t. The experiments show that the kinetics of coarsening of γ precipitates is much slower than that in the reverse system. This is consistent with behavior expected from diffusion in the two phases.

The Ni_3Ge phase behaves similarly to Ni_3Al in that it can be aged to produce disordered precipitates of the Ni-Ge solid solution from Ni_3Ge matrix. We do not yet know if this is also true for Ni_3Ga, but preliminary experiments suggest that it is not.

ACKNOWLEDGMENTS

The authors express their appreciation to the National Science Foundation for financial support of this research under Grant # DMR-0209260.

REFERENCES

1. M.M.P. Janssen, *Metall. Trans.* 4;1623 (1973).
2. J.D. Verhoeven, J.H. Lee, F.C. Laabs and L.L. Jones, *J. Phase Equil.* 12;15 (1991).
3. C.C. Jia, Thesis Tohoku (1990), cited by H. Okamoto, *J. Phase Equil.* 14;257 (1993).
4. M. Watanabe, Z. Horita, D.J. Smith, M.R. McCartney, T. Sano and M. Nemoto, *Acta Metall. Mater.* 42;3381 (1994).
5. L.R. Cornwell and G.R. Purdy, *Metall. Trans.* 5;780 (1974).
6. W. Liu, H. Rösner and E. Nembach, *Z. Metallkde* 88;648 (1997).
7. A.J. Ardell and R.B. Nicholson, *Acta Metall.* 14;1295 (1966).
8. A. Maheshwari and A.J. Ardell, *Scripta Metall.* 26;347 (1992).
9. A. Maheshwari and A.J. Ardell, *Phys. Rev. Lett.* 70; 2305 (1993).
10. A. Maheshwari and A.J. Ardell, *Acta Mater.* 40;2661 (1992).
11. Y. Ma, J. Joshi and A.J. Ardell, *XI International Materials Research Congress*, Cancun, Mexico (2002), to be published.
12. Y. Ma, J. Joshi and A.J. Ardell, to be published.
13. M.E. Thompson, C.S. Su and P.W. Voorhees, *Acta Metall.* 42;2107 (1994).
14. A.J. Ardell, *Modelling Simul. Mater. Sci. Eng.* 8;277 (2000).
15. I.M. Lifshitz and V.V. Slezov, *J. Phys. Chem. Solids* 19;35 (1961).
16. C. Wagner, *Z. Elektrochem* 65;581 (1961).
17. H.A. Calderon, P.W. Voorhees, J.L. Murray and G. Kostorz, *Acta Metall.* 42;991 (1994).
18. J.R. Manning, *Acta Metall.* 15;817 (1967).
19. M. Koiwa and S. Ishioka, *Phil. Mag. A* 48;1 (1983).
20. A.J. Ardell, *Interface Sci.* 3;119(1995).
21. K. Fujiwara and Z. Horita, *Acta Mater.* 50;1571 (2002).
22. A.J. Ardell, *Scripta Metall.* 24;343 (1990).

AN ATOMIC SCALE STUDY OF THE PHYSICAL PROPERTIES OF DELTA PLUTONIUM AND Pu:Al ALLOYS

Bruno Siberchicot[1], Gregory Robert[1], Johann Bouchet[1]
and Alain Pasturel[2]

[1]CEA, Département de Physique Théorique et Appliquée
BP 12, 91680 Bruyères-le-Châtel, France.
[2]Laboratoire de Physique Numérique, CNRS,
25 avenue des Martyrs, BP 106, F38042 Grenoble, France.

INTRODUCTION

Plutonium is probably the most intriguing metal in the whole periodic table. For instance, the Pu phase diagram at atmospheric pressure has six stable allotropes, some with very complex open structures (α and β : monoclinic) and others with close-packed structures (γ tetragonal and δ, δ', ε : cubic). No other element displays this complexity of polymorphism. Moreover, the phase transitions are accompanied by large volume changes, with a 25% difference between the cubic (fcc) δ phase and the room temperature monoclinic α phase. In contrast to this phase, which is brittle, the face-centered cubic δ phase is ductile, a property that makes it convenient for engineering applications. Many other physical properties are puzzling like specific heat coefficients or electrical resistivity. The origin of these peculiar properties of metallic plutonium has generally been attributed to the fact that it marks the boundary between the itinerant and the localized *5f* electron systems. From thorium through neptunium, the atomic volume displays the parabolic decrease typical of transition metals as the number of bonding electrons increases. Then the volume of the actinides jumps up sharply from neptunium to americium, ascribed to the localization of the *5f* electrons. From a physical point of view the actinide series could be divided in two sub-series with very different characteristics. Plutonium is exactly located at the center of this discontinuity. The character of the *5f* electrons varies from nearly pure metallic (delocalization) in α-Pu, to varying degrees of localization in the elevated-temperature phases.

The δ phase of pure plutonium is stable from 593 K to 736 K. Small additions of group IIIB metals (Al, Ga, In or Tl) can stabilize this phase at room temperature but the low-temperature limit of the impurity solubility is not well known. The Pu-Ga phase

diagram by Chetobarev *et al.*[1] indicates an eutectoid decomposition of the high-temperature δ-phase into the α-Pu and Pu_3Ga. By contrast Ellinger *et al.*[2] report no such decomposition. Similar problems are reported for plutonium-aluminium alloys.

Moreover physics concerning plutonium and its alloys involves predicting its properties under long-term aging in both weapons and storage[3] environnement[4]. The knowledge of all plutonium properties is a major challenge and first-principles studies of pure plutonium, alloys, and finite temperature simulations are needed.

In a first part this paper reports on a study of the electronic structure of pure plutonium for three of its localized phases (δ, δ' and ε) and a finite temperature description of the related phase diagram in a second part. A third part deals with the calculation of solubility limit of aluminium in δ plutonium.

BAND-STRUCTURE CALCULATION RESULTS

The density-functional theory and its local-density approximation (DFT-LDA), which sucessfully describes light actinides underpredicts the δ-phase volume by about 35 %. δ-Pu is not the only material for which LDA fails to reproduce the ground-state properties ; Mott insulators, like *3d* transition metal oxides, and a great variety of materials whose electronic structure contains partially filled valence *d* or *f* shells are not correctly described. The failure of the standard LDA approach has led to attempts to go beyond LDA[5-7] for plutonium. It is well established that this deficiency is linked to the strong on-site repulsion U between electrons in the localized *d* or *f* states. In fact, correlation effects arise when U exceeds or equals the mean conduction bandwith W. Recently the so-called LDA+U approach[8] has been applied to the problem of δ-Pu[9-11]. In these calculations the Hubbard U is treated as an adjustable parameter to fit the calculations to the experimentally observed volume for δ-Pu. Bouchet *et al.*[10] have shown that this method stabilizes the fcc δ-phase versus the bcc one (Bain's paths), reproduces the correct order of elastic constants (C' >0 and negative Cauchy pressure) and improves the relative values of these constants. At the same time, Wang and Sun[12] obtained a correct equilibrium volume by using Generalized Gradient Approximation (GGA) and by considering an antiferromagnetic alignment of spins.

In order to have a general point of view of the effect of different approximations, we performed band-structure calculations for δ, δ' and ε-Pu phases within LDA, GGA and LDA+U in non-magnetic and antiferromagnetic (AF) configurations. The electronic structures and total energies are calculated using the accurate all-electron full-potential linearized augmented plane-wave (FPLAPW) method (WIEN2k[13]) with the von Barth functional and Perdew-Wang 91 for GGA calculations. The relativistic Dirac equation is solved self-consistently for core states and the scalar relativistic one for valence states. Spin-orbit coupling is included, and *6p* local orbitals are used for a better treatment of $6p_{1/2}$ and $6p_{3/2}$ states. For LDA+U calculations the atomic value of 3.13 eV for U has been used.

For δ-Pu, although in the non-magnetic case GGA does not really improve equilibrium properties (volume and bulk modulus), the AF configuration leads to an equilibrium volume close to the experimental one. On the contrary a ferromagnetic order

gives a too large volume. Nevertheless, in both cases, ferro and AF, GGA leads to a net magnetic moment of about 2 μ_B per atom in contradiction with experiments. LDA+U also leads to correct equilibrium properties, but moreover, in AF as well as ferromagnetic configuration a perfect cancellation of spin and orbital moment per atom is obtained. This result is in better agreement with scarce experimental data. For a given cristallographic structure, in all cases the more stable state is always obtained for an antiferromagnetic alignment of spins. The main results for AF configurations are displayed in table 1. These results open two main questions : (i) why does GGA give such differences between non magnetic and AF configurations, (ii) do an antiferromagnetic or a more complex magnetic order really exist for the localized phases of plutonium ? According to our results and scarce experimental features, a more probable magnetic configuration for plutonium may be spin-glass like. New calculations in a disordered local moment framework should be a next step toward a better knowledge of plutonium physics.

Table 1. Results of calculations

	Experiment			LDA (T= 0 K)		
	850K	750K	650 K			
Phase	BCC	BCT	FCC	BCC	BCT	FCC
V_0 (A^3/atom)	24.29	24.79	24.91	16.54	19.94	20.02
Bulk modulus GPa	21 (a)	27 (a)	29 (a)	70	70.5	71
Magnetic order	PM	PM	PM	AFM	AFM	AFM
Mag. Mom./ atom (μ_B)	0	0	0	0.38	1.95	1.89
Cohesive Energy (eV)	3.7 (b)	3.8 (b)	3.8 (b)	6.509	6.284	6.269
E_{FCC} -E_{BCT}(eV)				- 15 meV		
E_{BCT} -E_{BCC}(eV)				- 240 meV		
Phase order	FCC → BCT → BCC			BCC → BCT → FCC		

GGA (T= 0 K)			LDA+U (T= 0 K) U= 3.13 eV		
BCC	BCT	FCC	BCC	BCT	FCC
22.61	24.20	24.42	23.95	24	24.05
40	54	55	52	68	66
AFM	AFM	AFM	AFM	AFM	AFM
2.03	2.23	2.29	0	0	0
4.90	4.977	4.981	5.26	5.29	5.3
4 meV			10 meV		
79 meV			59 meV		
FCC → BCT → BCC			FCC → BCT → BCC		

a) J.A. Cornet *et al.*, *JNM*, **28**, 303, (1968)
b) M. I. Baskes, *PRB*, 62, 15532, (2000)

PHASE DIAGRAM

Since we are treating high-temperature properties of δ-Pu, δ'-Pu and ε-Pu from calculations at 0K, a reliable thermodynamic model is needed. As Pu-3.6 at. % Ga alloy behaves like a Debye solid at ambiant pressure and low temperature[14], we chose to use the Debye model for plutonium instead of a classical mean-field approach. We first briefly summarize this model.

If we can calculate the Helmholtz free energy as an explicit function of volume and temperature, all other thermodynamic parameters can be derived. The free energy can be written as :

$$F(V,T) = E_c(V,T) + F_{ion}(V,T) + F_{el}(V,T) + F_{mag}(V,T)$$

$E_c(V)$ is the cohesive energy at OK derived from *ab initio* GGA and LDA+U antiferromagnetic calculations. For this analysis, binding curves are fitted to an exponential function mathematically equivalent to a Morse function[15]. $F_{ion}(V,T)$ is the vibrational energy calculated in the framework of Debye model :

$$F_{ion}(V,T) = -k_B T[D(\theta_D / T) - \ln(1 - \exp(-\theta_D / T))] + \tfrac{9}{8} k_B \theta_D$$

with θ_D the Debye temperature related to bulk modulus. $F_{el}(V,T)$ is the thermal electronic contribution :

$$E_{el}(V,T) = \int n(\varepsilon,V) f \varepsilon d\varepsilon - \int^{\varepsilon_F} n(\varepsilon,V) \varepsilon d\varepsilon$$

where f is the Fermi distribution. $F_{mag}(V,T)$ is the magnetic free energy[12]

$$F_{mag}(V,T) = -k_B T \ln[M_S(2L - M_S) + 1]$$

where M_S is the total spin magnetic moment and L is the *5f* orbital moment.

From the Helmoltz free energy versus volume curves, equilibrium lines between the three phases (δ-Pu, δ'-Pu and ε-Pu) are calculated and the phase diagram plotted. The corresponding GGA and LDA+U phase diagrams are reported in figures 2 and 3 and could be compared to the experimental pressure-temperature diagram drawn in figure 1.

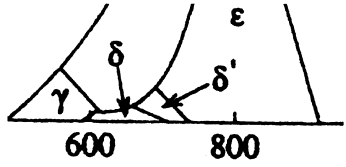

Figure1: Part of the phase diagram of plutonium

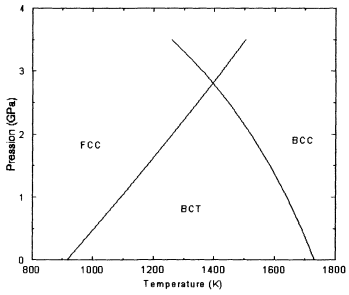

Figure 2. Phase diagram within GGA

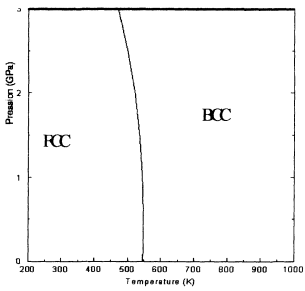

Figure 3. Phase diagram within LDA+U (U=3.13 eV)

Although the general shape of the diagram is reproduced within GGA, the absolute values of pressures and temperatures are dramatically too high. The main explanation comes from the large energy differences obtained between the three phases. LDA+U leads to a better phase diagram (only δ-Pu/ε-Pu equilibrium calculated up to now) although the reproduction of the experimental diagram is not perfect.

SOLUBILITY LIMIT OF δ-PLUTONIUM

As discussed in the introduction, the understanding of equilibrium between Ga and Pu_3Ga or Al and Pu_3Al with temperature is one of the main goal in the study of plutonium alloys. Given the crystal structure of an ordered compound, one can calculate its equilibrium properties and the more stable structure between a few possible different crystal forms at 0 K. However, it is necessary to treat solid solutions and to know the evolution of the structural stability as a function of temperature. In this study, the basic tool to determine such properties is based on a generalized three-dimensional Ising model.

The problem consists in the *ab initio* determination of the 3D Ising model parameters[16] and the study of this model at finite temperature.

The total energy of a disordered alloy A_xB_{1-x} can be described in terms of a convergent series of concentration-independent multisite interactions. For a given spin configuration α the total energy is expressed by :

$$E_{tot}^{\alpha}(r) = \sum_{\gamma}^{\gamma \max} J_{\gamma}(r)\xi_{\gamma}^{\alpha}$$

with $J_\gamma(r)$ is the concentation-independent multisite interaction associated with the multisite correlation

$$\xi_{\gamma} = \frac{1}{N_{\gamma}} \sum_{|n_j|} \sigma_{n_1}\sigma_{n_2}...\sigma_{n_{\gamma}}$$

σ_n equals +1 or –1 when the site is occupated by an atom A or B and N_γ is the number of γ-type clusters. Then, for a finite number of total energies associated with specific ordered structures :

$$J_{\gamma}(r) = \sum_{\alpha} (\xi_{\gamma}^{\alpha})^{-1} E_{tot}^{\alpha}(r), \phi < \gamma < \gamma_{\max} \text{ and } J_{\gamma}(r) = 0, \gamma_{\max} < \gamma < \infty$$

where ϕ is the empty cluster.

The parameters entering the Ising model are derived from first-principles calculations of total energies for a limited set of periodic crystal structures[17]. The following structures were considered : pure Pu and Al (A1 fcc), Pu_3Al and Al_3Pu ($L1_2$ simple cubic), Pu_3Al and Al_3Pu ($D0_{22}$ centered tetragonal), PuAl ($L1_0$ tetragonal and PuAl ($L1_1$ trigonal). We took into account interaction parameters for empty cluster $J_{0,1}$, point $J_{1,1}$, first-neighbor pair $J_{2,1}$, second neighbor pair $J_{2,2}$, three-body cluster $J_{3,1}$, and four-body cluster $J_{4,1}$ terms.

All calculations have been performed within LDA+U with the same value of U as used for pure δ-Pu (3.13 eV) in the framework of the full-potential linear-muffin-tin-orbital (FP-LMTO) method[18,19] with von Barth-Hedin exchange-correlation potential and spin-orbit coupling. We only present preliminary results where the antiferromagnetic configuration was not yet taken into account.

The results of formation energies

$$E_{Pu_xAl_{1-x}}^{f} = E_{Pu_xAl_{1-x}}^{\min} - (xE_{Pu}^{\min} + (1-x)E_{Al}^{\min})$$

are reported in table 2 and plotted in figure 4.